

Video Article

Receptor Autoradiography Protocol for the Localized Visualization of Angiotensin II Receptors

Andrea Linares¹, Leena E. Couling², Eduardo J. Carrera³, Robert C. Speth²¹Farquhar College of Arts and Sciences, Nova Southeastern University²Department of Pharmaceutical Sciences, College of Pharmacy, Nova Southeastern University³School of Medicine, University of ColoradoCorrespondence to: Robert C. Speth at rs1251@nova.eduURL: <http://www.jove.com/video/53866>DOI: [doi:10.3791/53866](https://doi.org/10.3791/53866)Keywords: Neuroscience, Issue 112, Receptor, Autoradiography, Cryostat, Brain Sectioning, X-ray, Film, Developing, AT₁R Binding, Angiotensin II

Date Published: 6/7/2016

Citation: Linares, A., Couling, L.E., Carrera, E.J., Speth, R.C. Receptor Autoradiography Protocol for the Localized Visualization of Angiotensin II Receptors. *J. Vis. Exp.* (112), e53866, doi:10.3791/53866 (2016).

Abstract

This protocol describes receptor binding patterns for Angiotensin II (Ang II) in the rat brain using a radioligand specific for Ang II receptors to perform receptor autoradiographic mapping.

Tissue specimens are harvested and stored at -80 °C. A cryostat is used to coronally section the tissue (brain) and thaw-mount the sections onto charged slides. The slide-mounted tissue sections are incubated in ¹²⁵I-SI-Ang II to radiolabel Ang II receptors. Adjacent slides are separated into two sets: 'non-specific binding' (NSP) in the presence of a receptor saturating concentration of non-radiolabeled Ang II, or an AT₁ Ang II receptor subtype (AT₁R) selective Ang II receptor antagonist, and 'total binding' with no AT₁R antagonist. A saturating concentration of AT₂ Ang II receptor subtype (AT₂R) antagonist (PD123319, 10 μM) is also present in the incubation buffer to limit ¹²⁵I-SI-Ang II binding to the AT₁R subtype. During a 30 min pre-incubation at ~22 °C, NSP slides are exposed to 10 μM PD123319 and losartan, while 'total binding' slides are exposed to 10 μM PD123319. Slides are then incubated with ¹²⁵I-SI-Ang II in the presence of PD123319 for 'total binding', and PD123319 and losartan for NSP in assay buffer, followed by several 'washes' in buffer, and water to remove salt and non-specifically bound radioligand. The slides are dried using blow-dryers, then exposed to autoradiography film using a specialized film and cassette. The film is developed and the images are scanned into a computer for visual and quantitative densitometry using a proprietary imaging system and a spreadsheet. An additional set of slides are thionin-stained for histological comparisons.

The advantage of using receptor autoradiography is the ability to visualize Ang II receptors *in situ*, within a section of a tissue specimen, and anatomically identify the region of the tissue by comparing it to an adjacent histological reference section.

Video Link

The video component of this article can be found at <http://www.jove.com/video/53866/>

Introduction

Cardiovascular disease continues to be the leading cause of death and disability in the United States, causing more than 30% of deaths in the U.S. in 2011¹. The most recent statistics from the American Heart Association indicate that more than one person in three has one or more type of cardiovascular disease. Cardiovascular research continues to make strides against understanding this disease, but as generations begin getting older it is imperative to continue these efforts. The Renin-angiotensin System (RAS) plays a central role in the regulation of the cardiovascular system primarily by promoting atherosclerosis, inflammation, systemic vasoconstriction, and activation of the sympathetic nervous system (**Figure 1**)²⁻⁸.

The RAS is a hormonal system that is activated when juxtaglomerular cells of the kidney secrete renin into the bloodstream in response to decreased blood pressure, increased sympathetic stimulation, or decreased sodium flow by the macula densa. Renin metabolizes angiotensinogen (synthesized in the liver) to form angiotensin I (Ang I). Ang I is then metabolized by angiotensin-converting enzyme (ACE), an ectoenzyme on the luminal side of vascular endothelial cells, primarily in the lungs and kidneys, to form angiotensin II (Ang II), the main effector peptide of the RAS. Ang II is capable of activating two receptor subtypes; the type 1 receptor (AT₁R) and the type 2 receptor (AT₂R), both which regulate the cardiovascular system, maintain fluid and electrolyte homeostasis and are now considered to affect cognitive function and neurodegenerative disease processes^{8,9}. A local, brain-specific RAS is reported to independently synthesize Ang II. In the brain, the precursor protein angiotensinogen is synthesized in astroglia¹⁰ converted to Ang I by a renin-like enzyme³, possibly prorenin bound to the prorenin receptor¹¹, and subsequently converted to Ang II by angiotensin-converting enzyme which is abundantly expressed on the extracellular surface of neurons in the brain¹². This intrabrain generated Ang II is the agonist for the brain AT₁ and AT₂ receptors that are isolated from blood-borne Ang II.

While the AT₁R plays an important physiological role, it is better known for its pathophysiological effects throughout the body, primarily affecting the cardiovascular system and kidneys (**Figure 2**). When Ang II binds to the AT₁R, it causes vasoconstriction; increasing resistance to blood flow and raising blood pressure. It also promotes the synthesis and secretion of aldosterone and vasopressin, leading to increased sodium and water retention. These effects can also induce ischemic brain damage and cognitive impairments and is linked to Parkinson's disease, Alzheimer's disease, and diabetes, as well as being recently identified to affect learning and memory¹³⁻¹⁵. There is a feedback loop in the RAS in that AT₁R on the juxtaglomerular cells in the kidney inhibits renin secretion. Interestingly, the AT₂R generally counter-regulates the action of AT₁R, causing vasodilation, neurite outgrowth, axonal regeneration, anti-proliferation, and cerebroprotection among many others¹⁶⁻²⁰. The AT₂R has also been identified as a target for anti-hypertension and recently, anti-cancer drugs²¹. Determining the localization and density of Ang II receptors within various tissues and how they are impacted by various treatments and disease states using quantitative densitometric receptor autoradiography will help uncover the role the RAS plays in specific diseases.

Receptor autoradiography has been used for over 30 years as an effective method for indicating the presence of angiotensin II receptors and other components of the RAS in the brain and other tissues of the rat, mouse, guinea pig, dog and human under a variety of experimental conditions²²⁻³⁴. The importance of locating Ang II receptors within the brain is that one can apply functional neuroanatomy to the actions of Ang II in the brain, *e.g.*, the presence of AT₁R in the paraventricular nucleus of the hypothalamus (PVN) suggests a function of Ang II in the brain to stimulate vasopressin, oxytocin or corticotropin releasing hormone (CRH) release, or activation of the sympathetic nervous system. Thus, drugs that block the AT₁R might decrease some of these PVN-mediated effects associated with over activity of the brain RAS. Work in progress suggests that the use of AT₁R antagonists can decrease Post-traumatic Stress Disorder (PTSD)-induced release of CRH and ameliorate the symptoms of PTSD (Hurt *et al.*, submitted for publication). The PVN, subfornical organ (SFO), and amygdala are known for regulating homeostasis, appetite/thirst, sleep, memory, emotional reactions, and are the target areas of this demonstration study. These regions were examined by collecting coronal sections of a brain on microscope slides, and treating the sections with specific inhibitors along with a specific radioligand for Ang II receptors. In this study, all materials and reagents along with suggested vendors are listed, Iodine-125 was used to radiolabel an Ang II receptor antagonist, sarcosine¹, isoleucine⁸ Ang II (SI Ang II), which was then purified as the mono¹²⁵I-SI Ang II using HPLC methods as described previously³⁵. The use of this high specific activity radioligand allows the visualization of areas of low, moderate and high receptor density after exposure of the radiolabeled sections to x-ray film. By calibrating the film with brain paste standards containing known amounts of Iodine-125, the specific amount of Ang II receptor binding in an area can be quantified. In experimental studies, the Ang II receptor binding in the brains of experimental subjects can be compared to that in the brains of control subjects. This can indicate whether the actions of Ang II are altered in response to a genetic condition, phenotypic abnormality, disease state or drug treatment. This knowledge can then be applied to the development of therapies to treat diseases associated with dysregulation of the RAS. Alternative techniques that identify receptor binding sites, but with reduced anatomical resolution, are binding assays that use tissue membrane preparations derived from tissue homogenates, which are incubated with the radioligand over a range of concentrations to assess radioligand binding affinity as the dissociation constant (K_D) and maximal binding capacity (B_{max}) of the tissue of interest.

The protocol described here can be broken down into 5 major components: Preparing Tissue Sections for Receptor Autoradiography; Receptor Autoradiography; Film Exposure and Development; Histology; and Densitometric Image Analysis.

Protocol

All animal procedures carried out for this study were approved by the Institutional Animal Care and Use Committee of Nova Southeastern University in accord with the Guide for the Care and Use of Laboratory Animals, 8th Edition (The National Academies Press, Washington, DC, 2011).

1. Preparing Tissue Sections for Receptor Autoradiography

1. Upon sacrifice, harvest fresh brain tissues, and wrap in aluminum foil and place in a -20 °C freezer as soon as possible. To maintain the correct shape, place brains in a brain mold that simulates the inside of the skull, wrap in aluminum foil and place in a -20 °C freezer. After 30 min, place tissues in a sealable freezer storage bag and move to a -80 °C freezer for long-term storage.
 1. Obtain the fresh frozen tissue specimen of interest from the -80 °C freezer, and transfer to a cryostat set to a minimum of -10 °C and maximum of -18 °C, to avoid thawing.
 2. Place the specimen onto the tissue mount with a glycol and resin-based embedding medium, only embedding a small part of the specimen into the medium. For brain, the brain is mounted vertically to enable sectioning in the coronal plane.
2. Place the tissue mount onto the microtome within the cryostat and firmly tighten in place. Ensure the left and right side of the brain are in the same antero-postero coordinates, and that the dorso-ventral axis is perpendicular to commonly used brain atlases.
3. Begin cutting at the desired thickness (20 μm recommended) and thaw mount the sections onto microscope slides in a vertical direction to have a greater surface area of space in the slide. Collect sections onto slides in sequential sets of five, *i.e.* the first set of slides are labelled 1-1, 1-2, 1-3, 1-4, and 1-5 (**Figure 3**).
4. After filling a set of slides with sections, allow slides to air dry for up to 1 hr, then place the slides in a plastic slide box in a self-sealing freezer storage bag, and store at -20 °C.

2. Receptor Autoradiography

CAUTION: Radioactivity. Use protective attire to handle radioactivity. Disposal is depended upon establishment, and must follow guidelines to properly decay (half-life 60 days) or be picked up by a certified company.

1. Remove the "-1" and "-2" slides of interest from the -20 °C freezer and mount into slide grips (**Figure 5**). Mount the "-1" slides together for 'non-specific' treatment, and the "-2" slides for 'total' treatment. 'Non-specific' jars will contain 10 μM final concentrations of PD123319 an AT₂R antagonist, and losartan an AT₁R antagonist, in assay medium buffer (AM5) (**Table 1**), the 'total' binding jars will only contain 10 μM PD123319 in AM5.

2. Invert the slide grips to place the slides into the pre-incubation Coplin jars filled with 35-40 ml of AM5, and respective inhibitors for 30 min at room temperature. Start subsequent sets in their pre-incubation bath at 4 min intervals.
3. Immediately transfer slides from the pre incubation solution to the incubation slide mailers, containing 10 ml of AM5, plus a predetermined concentration of ^{125}I -SI-Ang II (calculated in **Figure 4**) with the respective inhibitors, for 60-90 min at room temperature. If there is sufficient radioligand, 10 slides can be placed (back to back) in modified slide grips and incubated with ^{125}I -SI-Ang II in Coplin jars.
4. Place slides back into the slide grips (if needed), blot, and rinse by gently swirling for 1-2 sec in 400 ml of distilled water in two separate containers.
5. Transfer the slides sequentially into four Coplin jars containing 35-40 ml of AM5 for exactly 1 min each (as illustrated in **Figure 4**).
6. After the last 1 min rinse, gently swirl the sections for 1-2 sec in four changes of ice cold distilled water.
7. Blow-dry the slides with cool air (Caution: hot air volatilizes the radioactive compound) using four hair dryers set up from different angles for 4 min (**Figure 5**), until all the sections are dry, then place on a paper towel.
8. Mount slides with tissues facing up onto a cardboard for apposition to X-ray film using double sided tape.
9. Mount at least one, ^{125}I iodine calibration standard slide onto each cardboard (**Figure 6**).
Note: Calibration standards consist of brain paste thoroughly mixed with ^{125}I iodine bound to a compound containing a phenol ring, compacted by centrifugation in a 1 ml tuberculin syringe, that are cryostat sectioned at the same thickness as the brain sections and thaw-mounted onto microscope slides. Alternatively, ^{125}I calibration standards in plastic resin sectioned at 20 μm thickness can be obtained commercially. The plastic resin in these standards partially shields the film from the radiation such that a tissue equivalency of ~40% should be factored into the calibration.

3. Film Exposure and Development

1. Proceed to a darkroom with a strap-back X-ray cassette and autoradiography film. Open the cassette and place the cardboard with slides inside (**Figure 6**).
 1. Turn the lights off and turn on the safelight. Carefully open the box of X-Ray film, remove one film, and place the film shiny side up (with the jagged edge on the bottom right corner) on top of the slides in the cassette. Carefully close the cassette, and twist the locking bars to seal out light (**Figure 6**). Expose the slides for several days to several weeks at -20 °C.
2. In the darkroom, open the cassette and proceed with the film developing process.
 1. Place the slides into the trays consecutively; developer for 2 min, water containing 5% glacial acetic acid for 30 sec, and fixer for 5 min. The films are placed into a tray with running water for 20 min, then placed into Photoflo for no more than 10 sec and hung.
Note: The exposure time is determined empirically and can involve multiple films with different exposure times: long enough to obtain measurable signals from areas with low binding, but not so long as to saturate the film by areas with high binding. Once acceptable exposures are obtained, then proceed to the next step.

4. Histology

1. Prepare the thionin stain and staining reagents (**Table 2, Figure 7**).
 1. Place the "-3" slides in the slide rack, and transfer in sequential order beginning with deionized water for 1 min, then thionin stain solution for 10 min followed by three dips into deionized waters, and one 30 sec wash in deionized water.
 2. Following the water, place the slide rack into ethanol washes as follows; 50%, 70%, and 90% for 30 sec, followed by two ethanol washes at 100% for 1 min each. Lastly, place the slide rack into xylene for 3 min, then transfer over to a second xylene solution for 5 min.
2. Remove one slide at a time from the last xylene bath, and cover the upper edge of the slide with a resin base in organic solvent mounting medium, and place a 24 mm x 60 mm coverslip onto the slide. Allow slides to sufficiently dry for ~48 hr and then scan into the computer at 2,400 dpi grayscale.

5. Densitometric Image Analysis

1. Place the film shiny side down, with the jagged edge on the bottom left corner and scan using a proprietary scanner capable of transmitting the film density information without any distortion in the imaging system computer.
2. Open the proprietary imaging system and utilize the calibration bars to establish calibration standards for future densitometric analysis of the images on the film (**Figures 9-12**).
3. Measure areas of interest by either establishing a template or empirically outlining the areas of interest. Data is collected and separated based on film, either control or wild type (section), and region. Make sure to include density (fmol/g), scan area, and total target area in measurements (**Figure 9**).
 1. Adjust scan area bars by assuring that region of interest falls between parameters of highlighting (**Figure 10**).
 2. Export data into a spreadsheet (**Table 4**). Multiply the density times the total target area, then divide by the scan area in order to obtain the value for the binding of that specific area. Once this is done to all values measured, subtract the established non-specific from total to yield the specific binding present. Averages may also be performed for these values.

Representative Results

The overview of the metabolic pathway of the Renin-Angiotensin System is shown in **Figure 1** and the direct focus on the Angiotensin II receptor subtypes (AT_1R and AT_2R) is described in **Figure 2**. **Figure 3** displays the transfer of coronal brain sections onto microscope slides, which are then run through a receptor autoradiography procedure using a predetermined ^{125}I -SIAng II concentration as seen in **Figure 4**. **Figure 5** illustrates the drying step for the slides in the receptor autoradiography which are then affixed onto a cardboard as seen in **Figure 6**, and subsequently developed. **Table 2** lists the reagents used for the thionin staining procedure for the slide-mounted tissue sections described in **Figure 7**. Calibration standard units for quantification are determined based on the date of the assay as seen in **Table 3**. **Figure 8** shows the establishment of a standard curve relating ^{125}I concentration (fmol/g tissue) to film exposure (relative optometric density). **Figure 11** illustrates the distinction between 'NSP' and 'total' groups, as well as the tissue labels, while **Figure 10** describes the setting of the threshold to a near zero value to obtain an accurate average value for the entire scanned area (Scan Area-pixel). **Table 4** displays the quantification process of obtaining specific binding based on subtracting the 'non-specific' from 'total' values. 'Non-specific' binding which contains losartan and/or PD123319 is created by the amount of radioligand bound to non- AT_1 , or AT_2 receptors. All of the radioligand bound to AT_1 receptors in the presence of PD123319 yields the 'total' binding. **Figure 11** displays the final measured areas of the PVN in total vs. non-specific binding adjacent to a thionin stained section for the anatomical confirmation of the PVN.

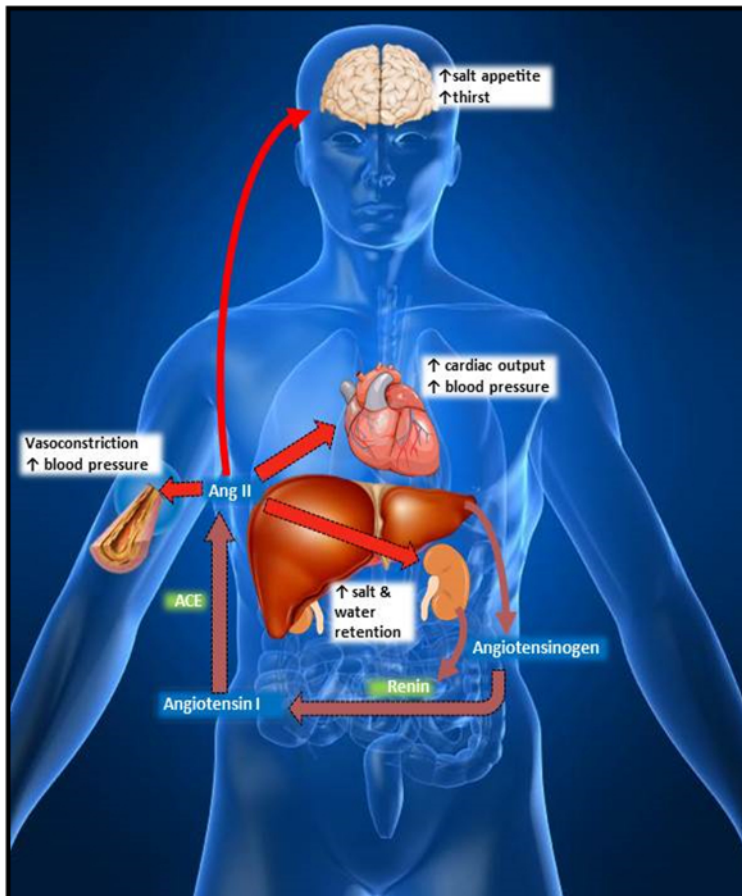


Figure 1: Metabolic Pathway of the Renin Angiotensin System (RAS) in the body. The liver releases the zymogen angiotensinogen, which is cleaved by kidney-secreted renin, forming Angiotensin I. Angiotensin converting enzyme (ACE) converts Ang I into angiotensin II (Ang II), the main precursor of cardiovascular disease. Ang II causes vasoconstriction, and increases blood pressure, cardiac output, salt appetite, thirst, and water retention. [Please click here to view a larger version of this figure.](#)

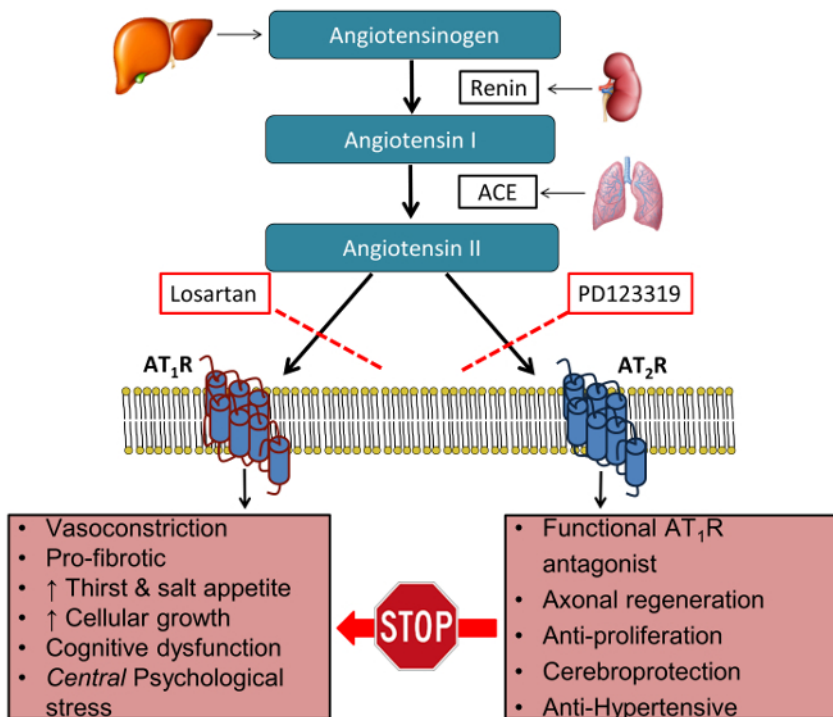


Figure 2: Functions of the Angiotensin type 1 and 2 receptors (AT₁R, AT₂R). AT₁R pathologically affects cardiovascular disease, directly acts to increase thirst and salt appetite, and exerts many other peripheral cellular activities as well as central psychological effects. AT₂R is a physiological antagonist of the AT₁ receptor, assisting in the efficacy of AT₁R antagonists³⁶ thereby having beneficial effects on vascular structure. [Please click here to view a larger version of this figure.](#)

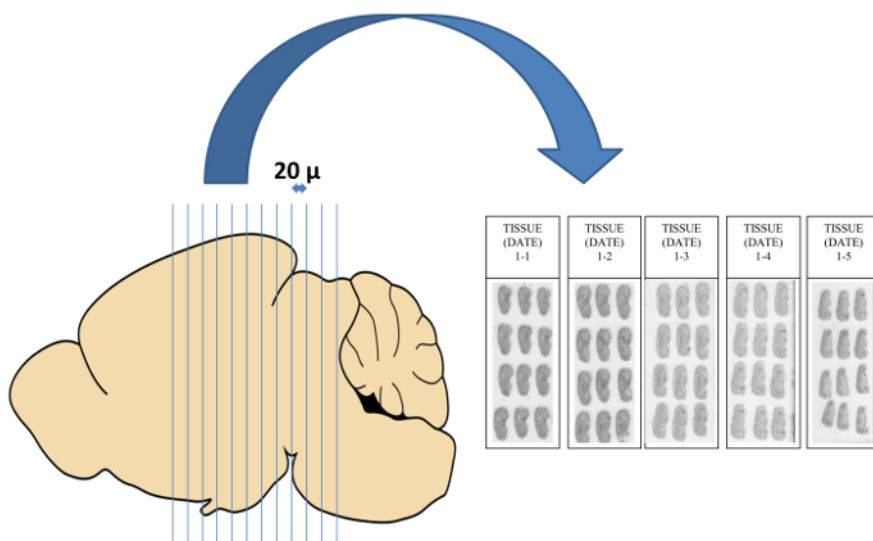


Figure 3: Cryosectioning of brain onto microscope slides at 20 µm thickness. Depending upon the temperature of the cryostat, the sections will at times display folds, cracks, curling, or become compacted on the microtome blade or knife holder. In such cases the section is discarded and a note is made to indicate that an extra 20 µm will separate this section from the previous section. Sections should be collected on slides in a vertical direction in order to maximize the total area needed to fill up a slide and therefore collect the greatest amount of sections on each slide. [Please click here to view a larger version of this figure.](#)

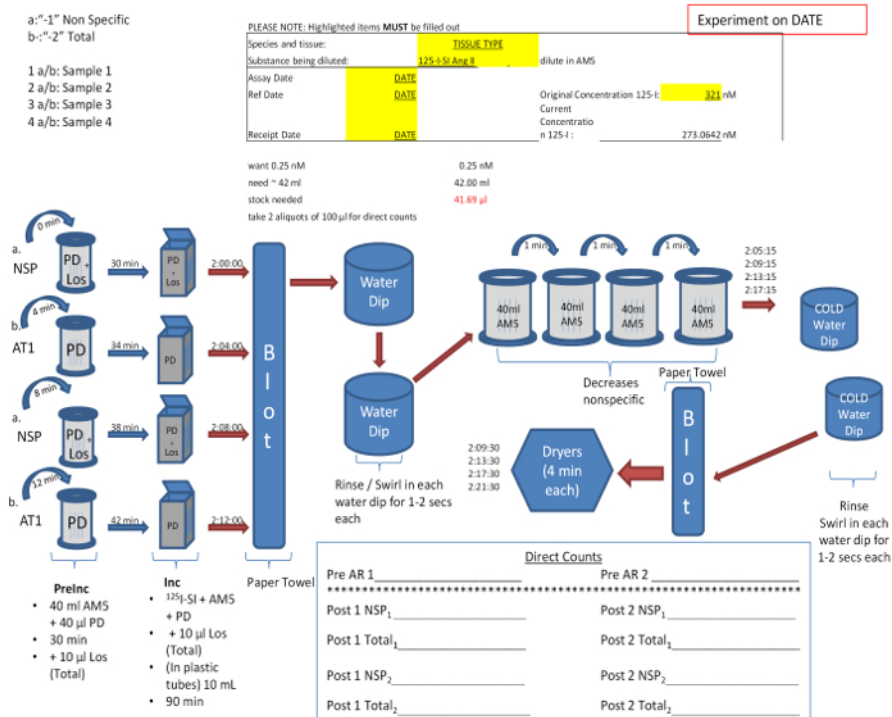


Figure 4: Sample of Experimental Design & Protocol for Receptor Autoradiography. Differentiation of 'total' (-2) and 'non-specific' (-1) directly relates to the presence and absence of receptor subtype antagonist. Protocol may vary based on the number of slides, and will increase by increments of 2 for each pair of total and non-specific slides. Radioligand concentration, previously determined is obtained by dilution of the stock into AM5. This solution is then evenly distributed to the incubation containers. Direct counts are taken before and after incubation to establish the exact concentration of the radioligand. [Please click here to view a larger version of this figure.](#)

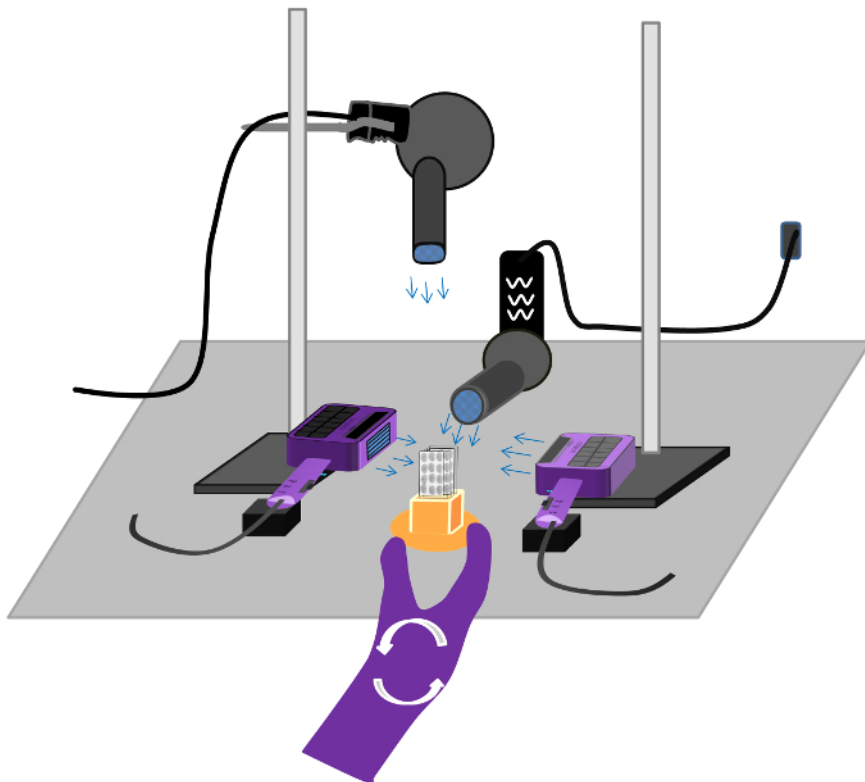


Figure 5: Configuration for drying station in receptor autoradiography. Drying times will vary based on the efficiency of the blow dryers as well as the ability to blot away any excess water after the last rinses. Slides will be dried once the section turns from clear to white. If slides are not fully dried then the radioligand can diffuse away from the receptor producing a fuzzy image that is not specific for the receptor binding sites. [Please click here to view a larger version of this figure.](#)

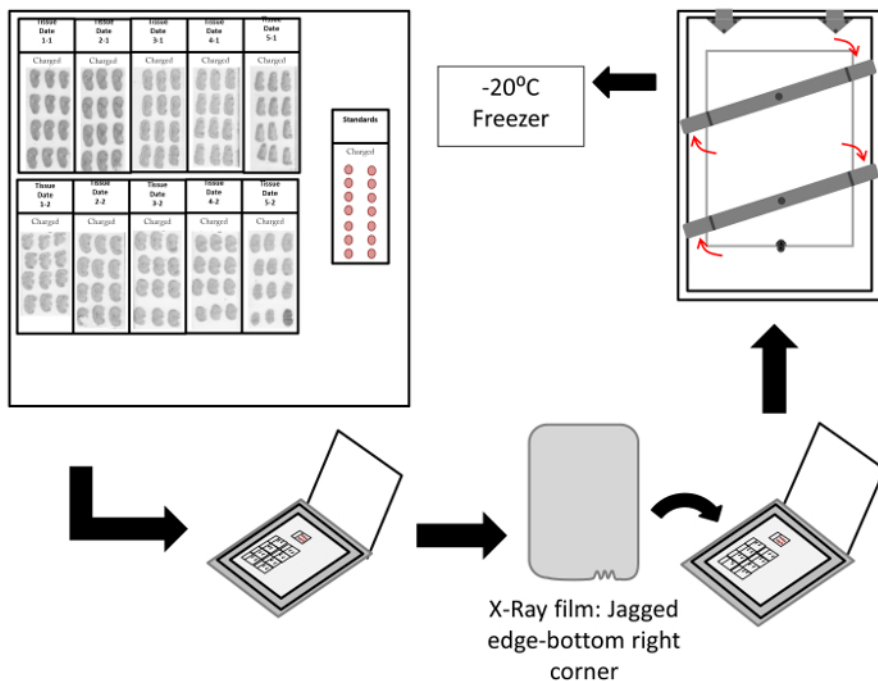


Figure 6: Exposing treated slides to x-ray film using a specialized cassette. Slide set-up is recommended to follow a pattern where comparison of both groups is facilitated. [Please click here to view a larger version of this figure.](#)

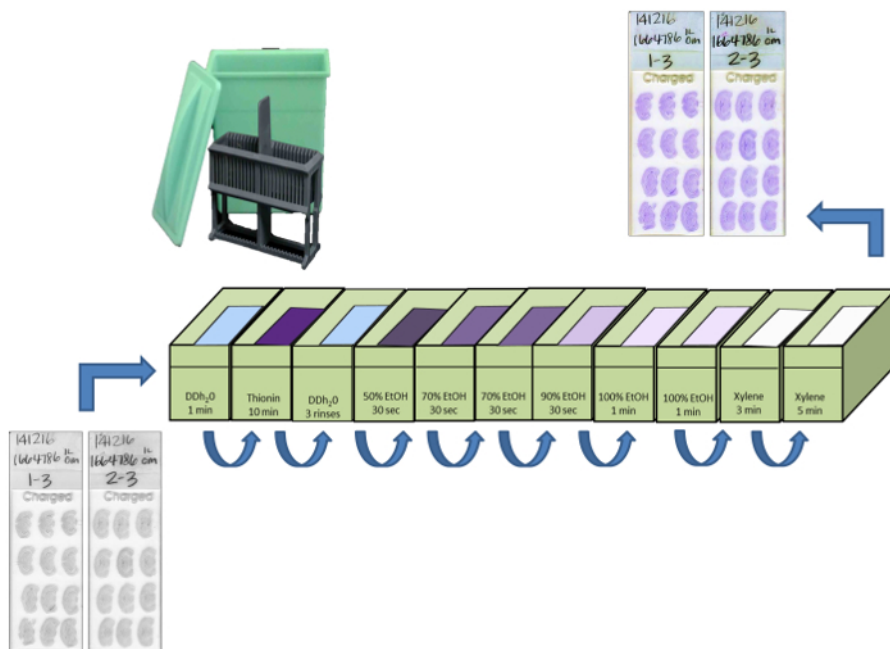


Figure 7: Set-up for Thionin Staining. Slides are loaded into a slide holder and immersed into sequential solutions. Timing allows for effective staining of the Nissl substance (rough endoplasmic reticulum) of neurons. A mounting medium application to the slides following dehydration allows for fixing of the coverslip to the slide, preserving the sections for comparative analysis. [Please click here to view a larger version of this figure.](#)

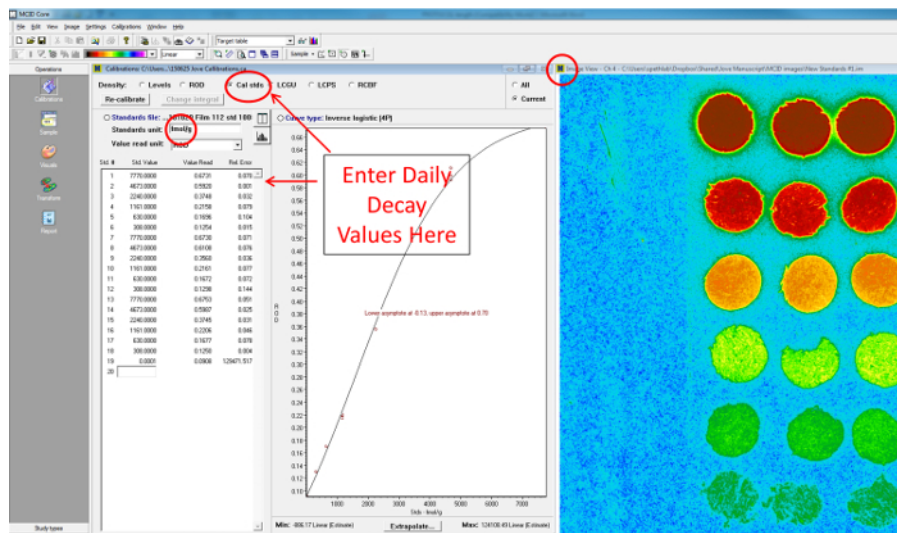


Figure 8: Setting the calibration standard. Each film contains its individual calibration standards, based on the brain paste and the time at which the experiment was done. A regression line describing the best fit values is generated by a proprietary imaging system program for the measured brain paste standards. This converts the relative optometric density (ROD) value from the calibration standards (cal stds, in red oval) to units of radioligand binding, in this example the units (fmol/g, circled in red) are femole radioligand bound per gram of wet tissue weight (fmol/g). The measurement of the brain paste standards is done with the circular tool and placed in the middle of the sample shown on the right in pseudocolor using the image view icon (circled in red). The circle to measure the calibration standard does not have to cover the whole sample, but rather measure an even area of the standard. [Please click here to view a larger version of this figure.](#)

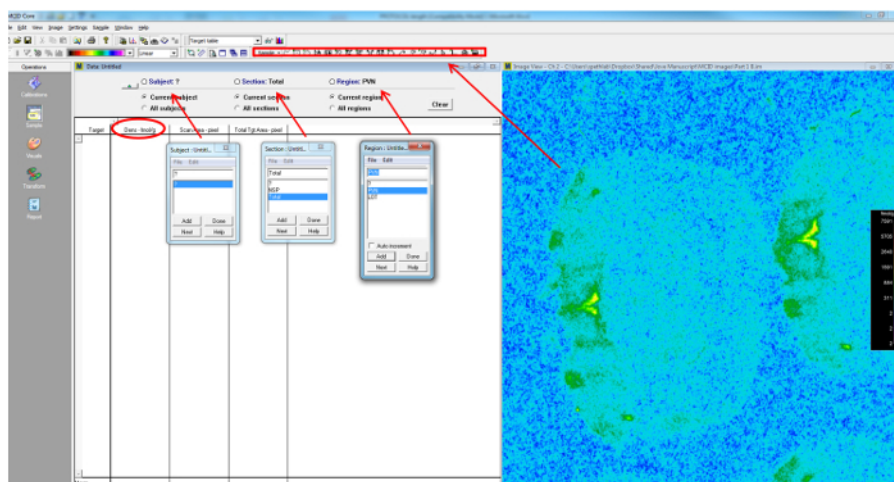


Figure 9: Identifying groups by sample number, non-specific/total, and regions for sample readings. Because multiple brains, brain regions, and multiple experimental groups are quantified together, it is crucial to differentiate between all of the factors. The subject indicates the brain sample and can also indicate group; the section indicates whether it is non-specific (NSP) or total, while the region allows the identification of multiple brain regions that are being sampled. The sample tool bar (red rectangle) describes different sampling tools, e.g., circle, square, template, freehand, eraser; that can be used to delineate area to be measured. The ROD values obtained within the area of the sampling tool are recorded on the spreadsheet as converted units of binding, fmol/g (circled in red). In addition, the total scan area within the sampling tool is recorded in the "Scan area-pixel" column while the total target area (the number of pixels that exceed the threshold value (described in Figure 10 legend) is recorded in the "Total Tgt Area-pixel" column. [Please click here to view a larger version of this figure.](#)

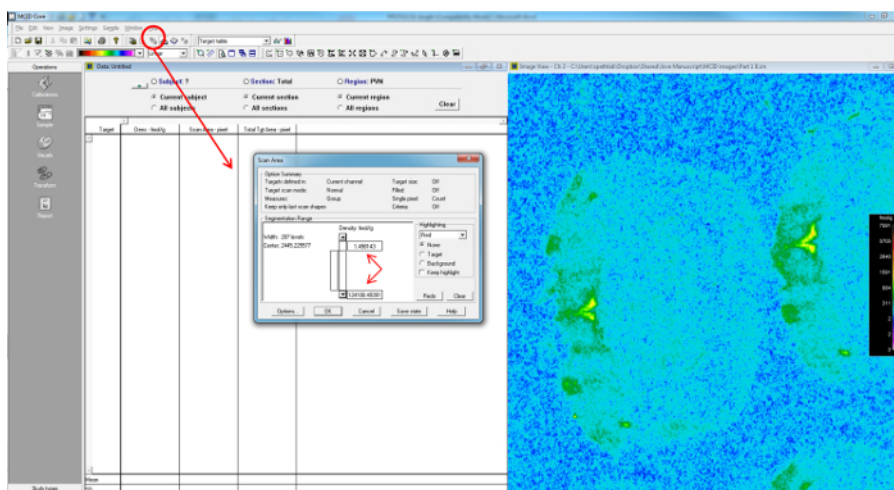


Figure 10: Determination of threshold for samples to be measured based on the standards. The scan area is unique for each film, and depends on the standards set. Using the thresholding tool (circled in red) to set threshold values for the density range for the scan area in fmol/g will allow for the areas measured (delineated by diagonal arrows) to fall between a range of 0, up to a point where the calibration curve begins to asymptote indicating that the film is nearing a maximal exposure, beyond which additional ¹²⁵I will cause no further increase in film density. Only pixels with film density greater than the lower threshold value are recorded in the "Total Tgt Area-pixel" column. Pixels with values less than the threshold value are assigned a value as close to zero as possible for determination of the average values of the entire scan area "Scan Area-pixel". [Please click here to view a larger version of this figure.](#)

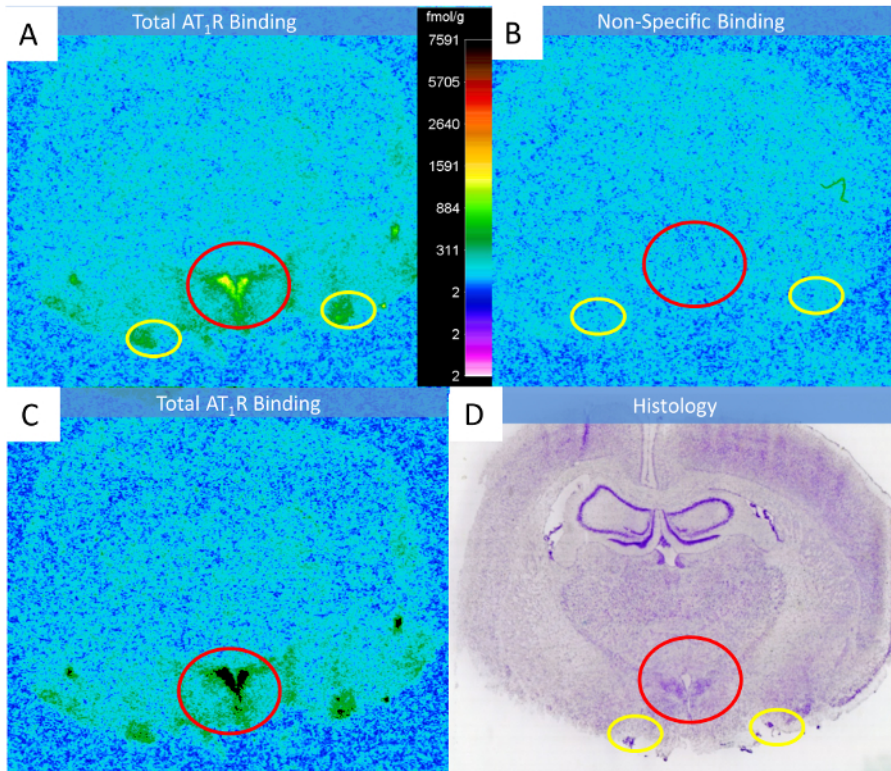


Figure 11: Representative images of receptor autoradiography binding to coronal sections of a female spontaneously hypertensive rat (SHR) at ~1.8 mm caudal to Bregma, displaying the paraventricular nucleus of the hypothalamus (PVN) and the bed nucleus of the accessory olfactory tract (BAOT). (A) Total binding of AT₁R binding (Red- PVN, Yellow- BAOT). (B) Non-specific binding with losartan (AT₁R antagonist) and PD123319 (AT₂R antagonist). (C) Total binding of AT₁R binding with an arbitrary threshold setting such as to delineate the shape of the PVN (black fill) exceeding the threshold value within the Scan Area which is recorded as Total Tgt Area). (D) Thionin stained section for anatomical confirmation of the structures showing high total binding, and for comparison with other brain regions or other experimental groups. [Please click here to view a larger version of this figure.](#)

Reagents	Amount
NaCl	8.76 g
Na ₂ EDTA	1.86 g
Bacitracin	141 mg
500 mM Dibasic Na ₂ PO ₄	100 ml
Distilled Deionized Water	900 ml
Adjust pH to 7.1 to 7.2 with NaOH or HCl	

Table 1: Assay Medium (AM5). Chemical components of the buffer used in tissue preparation.

Thionin Stain:	
180 ml distilled H ₂ O	} (pH this buffer solution to 4.3)
9 ml Sodium Acetate Solution, 1.0 M	
21 ml Acetic Acid Solution, 1.0 M	
Add 18 ml of 0.5% Thionin Solution	
1.0 M Sodium Acetate Solution	16.4g Sodium Acetate (anhydrous) dissolved in 200 ml distilled H ₂ O.
1.0 M Glacial Acetic Acid Solution	12.2 ml Glacial Acetic Acid to 200 ml distilled H ₂ O
0.5% Thionin Solution	0.5 gm Thionin in 100 ml distilled H ₂ O

Table 2: Thionin Stain Reagents. The thionin stain is made up of distilled water, 1.0 M Sodium Acetate and 1.0 M Glacial Acetic Acid solution, titrated to a pH of 4.3 prior to adding a 0.5% thionin solution.

				Days past reference date					
	Batch	fmol/g wet weight		Ref Date	1	2	3	4	5
Standard	nCi/mg	fmol/g	dpm/g	fmol/g	fom/g	fmol/g	fmol/g	fmol/g	fmol/g
number	30-May	30-May	30-May	30-May	31-May	1-Jun	2-June	3-June	4-June
1	9,706	4,463	21,547,320	4,463	4,411	4,361	4,311	4,261	4,212
2	5,838	2,684	12,960,360	2,684	2,653	2,623	2,593	2,563	2,533
3	2,798	1,286	6,211,560	1,286	1,272	1,257	1,243	1,228	1,214
4	1,451	667	3,221,220	667	659	652	644	637	630
5	787	362	1,747,140	362	358	354	350	345	342
6	385	177	854,700	177	174	173	171	169	167

Table 3: Daily Decay Rate Calculations for Calibration Standards. A daily decay rate spreadsheet for the calibration standards will need to be created based on the dates on which the experiment was performed. This spreadsheet is based upon the first order rate constant with a half-life ($t_{1/2}$) of 60 days. $N = N_0 \cdot e^{-kt}$, where N = the concentration of ^{125}I , at time t relative to the concentration at time 0 (N_0), and $k = \ln 2/t_{1/2}$.

Paraventricular Nucleous of the Hypothalamus						
Section	Target	Density-fmol/g	Scan Area	Total Target Area	Total*	
Total	1	996	4,383	4,383	996	
Total	2	921	3,362	3,362	921	
Total	3	818	3,445	3,445	818	Specific Binding
Total	4	710	2,906	2,906	710	967
AVERAGE		861	3,524	3,524	861	895
763						
Section	Target	Density-fmol/g	Scan Area	Total Target Area	Non-specific*	678
NSP	1	53	3,072	1,737	30	826
NSP	2	52	2,959	1,455	26	
NSP	3	86	3,180	2,035	55	
NSP	4	53	3,293	1,995	32	
AVERAGE		61	3,126	1,805.5	36	
Bed Nucleus of the Accessory Olfactory Tract						
Section	Target	Dens-fmol/g	Scan Area	Total Target Area	Total*	
Total	1	439	3,632	3,632	439	
Total	2	435	3,632	3,632	435	
Total	3	355	3,632	3,620	354	
Total	4	435	3,632	3,631	435	Specific Binding
Total	5	342	3,632	3,630	342	414
Total	6	334	3,632	3,606	331	393
AVERAGE		390	3,632	3,625	389	321
394						
315						
Section	Target	Dens-fmol/g	Scan Area	Total Target Area	Non-specific*	320
NSP	1	49	3,632	1,846	25	360
NSP	2	64	3,632	2,362	42	
NSP	3	53	3,632	2,275	33	
NSP	4	64	3,632	2,339	41	
NSP	5	51	3,632	1,879	26	
NSP	6	41	3,632	966	11	
AVERAGE		54	3,632	1,945	30	
*Total and Non-specific are density units of fmol/g.						
Total = density * total target area/scan area						
Non-specific = density * total target area/scan area						
Total Target Area is pixels that exceeded the threshold value, set as close to 0.00 fmol/g as possible.						
Pixels not exceeding the threshold value receive a value of 0 for assessment of total density.						
Pixels not exceeding the threshold value receive a value of 0 for assessment of Non-specific density.						
Specific Binding is Total minus Non-specific binding expressed as density units of fmol/g.						

Table 4: Quantitative analysis of paraventricular nucleus of the hypothalamus and bed nucleus of the accessory olfactory tract. Imaging software exports data as a spreadsheet in fmol/g, scan area, and total target area in pixels. 'Non-specific' binding is subtracted from 'total' binding in order to obtain the specific AT₁ quantitative binding.

Discussion

The protocol described identifies the visualization of 'total' and 'non-specific' binding of the radioligand in adjacent sections of coronal sections of a rodent brain previously harvested and stored at -80°C , and can be readily applicable to virtually every tissue that has anatomically resolved substructures which display differential amounts of receptors or radioligand binding sites. The procedures described within the protocol are simple and the analysis is critical for correctly interpreting results. The $20\ \mu\text{m}$ thickness was determined to be optimal; if the section is too thick the non-specific binding will increase, making it difficult to resolve the binding of the radioligand to its target. If the section is cut thinner, it becomes difficult to successfully cut and save sequential sections without distortion. The optimal cutting temperature will vary slightly due to the nature of the tissue and the thickness of the sections and is usually determined empirically. Once contact is made between the blade and the tissue, the orientation of the specimen can be reviewed, and realigned by moving the tissue specimen back away from the blade, and reorienting the mounting ball. When cutting a rodent brain it is critical to ensure the left and right side of the brain are in the same antero-postero coordinates, and that the dorso-ventral axis is perpendicular to commonly used brain atlases. Slide sets are pre-labelled in order to conduct studies on adjacent sections of tissues. The first sets of 5 slides are labeled 1-1, 1-2, 1-3, 1-4, and 1-5. The first cut section goes on slide 1-1 in the upper left corner (this is the upper right hand corner of the slide when it is frosted side down); the second cut section goes on slide 1-2, etc. The fifth cut section goes on slide 1-5. The sixth cut section goes on slide 1-1 to the left of the first section. After the first set of slides is filled, start another set of 5 slides, labeled 2-1, 2-2, 2-3, 2-4, and 2-5. This cycle is continued as far back into the brain as necessary. The "-4" and "-5" slides are kept as a backup or to radiolabel a different receptor.

The receptor autoradiography protocol depends upon the radioligand used and the characteristics of the receptors being surveyed to determine the concentrations of buffers, salts and inhibitors. For measurement of the AT1 subtype of Ang II receptors in this procedure, a high-affinity Iodine-125 labeled ligand, $^{125}\text{I-Sar}^1\text{Ile}^8\text{-Ang II}$ ($^{125}\text{I-SI-Ang II}$); radiolabeled by Robert C. Speth, Ph.D. (Peptide Radioiodination Shared Resource, Georgetown University), which is also available commercially) is dissolved in AM5 buffer (**Table 1**); a sodium phosphate buffer with sodium chloride, EDTA and bacitracin. AM5 provides good protection of the radioligand from metallopeptidases and bacitracin-sensitive peptidases providing a physiological pH and NaCl concentration to optimize binding characteristics. Pre-incubation in AM5 exposes the tissue sections to peptidase inhibitors to minimize radioligand degradation, and also dissociates endogenous Ang II from the Ang II receptors. Losartan and PD123319, AT1R and AT2R antagonists, respectively, that saturate their target receptors are added at concentrations ($10\ \mu\text{M}$) to prevent the radioligand from binding to these receptors to assess non-specific binding and limit specific binding to the AT1 receptor, respectively. The desired concentration of $^{125}\text{I-SI-Ang II}$ for the assay is determined and the required dilution of the stock solution is determined from a spreadsheet of the radioisotope decay rate (see protocol **Table 3**). Optimally a concentration of radioligand approximating the K_D is used which would occupy 50% of the receptors present. However, because radioligands can be costly lower concentrations e.g. 10-20% of the K_D concentration can be used. This has a potential advantage of increasing the signal to noise ratio by reducing non-specific binding more than specific binding. However, longer exposure times are required to develop an image of the binding. As noted above (section 3.4), if the exposure obtained is over or under exposed, the slides can be re-exposed to a new film for a shorter and/or longer time to achieve the desired exposure.

Densitometric image analysis can be done by a proprietary imaging system that provides an extensive compendium of the applications for autoradiography as well as other applications. Calibration standards are in fmol/g of wet tissue weight (assuming a specific gravity of one for the tissue). Each standard set, along with a background will generate a standard curve. There are several curve-fitting algorithms with and without weighting available to generate a standard curve from the relative optometric density (ROD) values for the different calibration standards. Selection of the curve that best represents the data is done empirically as the subroutine for curve fitting does not provide relative error values for the different standard curves. At RODs up to ~ 0.6 , the standard curve is pseudolinear. However, the film begins to saturate beyond this point forming a curve that asymptotes around 0.8 to 0.9 ROD units. If the standards that are bracketing the samples are above 0.9 ROD units, it is recommended to re-expose the film for a shorter period of time to obtain more reliable values of fmol/g binding of the samples closer to the pseudolinear range of the standard curve. Values derived at this extreme of the standard curve will result in small differences in ROD for significantly larger differences in radioligand binding. Hence the ability to detect changes in binding decreases as the film approaches its saturation point.

For measurements of specific regions, recommended measures are 'Density' in fmol/g, 'Scan area' in pixels, and 'Total Target Area' in pixels (**Figure 9**). It is important to set a threshold value as close to zero as possible (**Figure 10**) because variations in film density or the arbitrary aspect of the standard curve derived from the calibration standards can sometimes give values less than zero. If such values are averaged for all the pixels in the Scan Area it would derive an artificially low value. The criteria used to identify areas with binding can be very subjective, so it is best to closely pair the control and experimental brains as much as possible to reduce the incidence of subjective errors. Another challenge is to decide how many sections to average to get a final reading. A good indication of sections to analyze can be determined by following an accepted rat brain atlas, along with the stained histology slides. The size of the sampling area can also be a problem. In order to compensate, a template can be established to correct for any size discrepancies. The treatment of the sections could also affect an area of the structure that has high binding and are to be considered during analysis. This requires an alternative use of the 'thresholding' tool in the proprietary imaging system to set a density range exceeding an arbitrary value so as to represent the anatomical characteristics of the brain region being sampled such as the paraventricular nucleus of the hypothalamus within a sampling tool that encompasses the region of interest (**Figure 11**, panel C). It is also possible to include the area measurement into the determination of the amount of binding. This can be done by multiplying the value for specific binding times the number of pixels that were measured. Pixels can be converted to metric units by imaging a ruler in two planes, or a rectangle of known dimensions. The number of pixels that correspond to the length or area of the rectangle can then be expressed in metric units. At 2,400 dpi resolution, $\sim 9,000$ pixels = $1\ \text{mm}^2$ in our system.

Although the use of radioactive ligands is no longer a widely used technique; it is one of the few ways to visualize the physical distribution of receptors within the tissue specimens themselves as functional (capable of binding its innate ligand). Additionally, it can quantitate the number of receptors to enable evaluation of changes in functional receptor expression between treatment groups, between different brain regions or other structures, between different strains of animals, or animals of different ages, etc. Alternative methods are available to characterize neuroanatomical aspects of AT₁ receptor expression, however, they have limited value. In situ hybridization of mRNA for AT₁ receptors does not always correspond with AT₁ receptor expression or distribution in the brain. While immunological techniques can approximate differences in

receptor expression based upon the intensity of the staining of tissue sections, it is not possible to generate a standard curve for staining to allow for a numerical determination of receptor expression. Receptor autoradiography also provides a level of specificity for receptors (or other targets that specifically bind radioligands) that cannot be guaranteed using immunological techniques. In 2009, a series of articles were published³⁷⁻⁴³ that questioned the validity of 49 antibodies that were being used to assess 18 different G protein-coupled receptors and a transient receptor potential (TRP) channel. In essence, antibodies labeled identical bands on western blots from wild-type and knockout mice for the receptors in question. Subsequently, several groups have made similar observations using commercially available AT₁ and AT₂ receptor antibodies⁴⁴⁻⁴⁹. The use of a bacterial artificial chromosome which generates a reporter molecule, e.g., green fluorescent protein, driven by the AT₁ promoter is an indirect means of determining the presence or absence of AT₁ receptor-expressing cells in mouse (but not rat) brains based upon their having a functional AT₁ receptor promoter⁵⁰. It is possible to count "positive cells" in microscopically identified brain regions, but not to quantitate changes in the intensity of expression of the AT₁ receptor in these regions. Thus at this time the only validated techniques that available to directly measure Ang II receptor expression are radioligand binding methods. And, if anatomical resolution of functional AT₁ receptor protein is needed at a microscopic level, receptor autoradiography is the only technique available for such direct measurement.

Receptor autoradiography is not without limitations. The major concern is that of meeting the requirements to use radioactive materials in a research setting. It is necessary to have a radiation safety program with strict guidelines in place to assure the safety of researchers who work with radioactive materials and the safe disposition of the radioactive materials. This escalates the cost of research using radioactive materials to a point that precludes their use in many research settings. Additionally, the cost of radioligands can be substantial. Thus a receptor autoradiography experiment in which a large number of slide-mounted tissue sections are incubated in containers of radioligand can use hundreds if not thousands of dollars of radioligand. Another limitation is that tissues must be frozen prior to sectioning on a cryostat, stored for a period of time, and quickly rinsed and dried after incubation with radioligand, all of which can impair the ability of the receptors or protein of interest to bind the radioligand. For ligands that have rapid association/dissociation kinetics, it may not be possible to retain the binding of the radioligand to the receptor during the time needed to rinse away non-specifically bound radioligand. Also, with low amounts of radioligand binding long periods of film exposure - one month or more - may be required before a measureable image can form on the film. Another challenge is that addition of iodine-125 to a ligand may impair the ability of the ligand to bind to its target receptor or protein due to steric hindrance. The use of a smaller molecule, e.g., tritium (³H) eliminates the problem of steric hindrance, but tritium has such low energy and low specific activity (relative to iodine-125) that it is extremely difficult to generate a film image for most receptor populations. In light of these issues, there are many situations in which receptor autoradiography is unable to identify receptors or other molecular structures of interest.

Despite its limitations, receptor autoradiography can identify specific structures within a tissue, e.g., brain regions altered in response to experimental variables compared to a normal control brain. This knowledge can help determine the role of the AT₁R for Ang II or other receptor or enzymes in the pathology of disease. This knowledge has valuable pharmacological implications, as it indicates areas to target for potential therapies.

Disclosures

Robert Speth has licensed antibodies to angiotensin II receptors to a commercial vendor and receives royalties from the sale of said antibodies. The other authors have nothing to disclose.

Acknowledgements

This work was supported by NIH Grant HL-113905

References

1. Mozaffarian, D. *et al.* Heart disease and stroke statistics--2015 update: a report from the American Heart Association. *Circulation*. **131** (4), e29-322, (2015).
2. Peart, W. S. The Renin-Angiotensin System. *Pharmacol Rev*. **17** 143-182 (1965).
3. Ganten, D. *et al.* Angiotensin-forming enzyme in brain tissue. *Science*. **173** (3991), 64-65 (1971).
4. Ganten, D., Fuxe, K., Phillips, M. I., Mann, J. F. E., & Ganten, U. in *Frontiers in Neuroendocrinology*. Vol. 5 eds W. F. Ganong & L. Martini) 61-99, Raven Press, N.Y., (1978).
5. Fyhriquist, F., Metsarinne, K., & Tikkanen, I. Role of angiotensin II in blood pressure regulation and in the pathophysiology of cardiovascular disorders. *J Hum Hypertens*. **9 Suppl 5** S19-24 (1995).
6. von Bohlen und Halbach, O., & Albrecht, D. The CNS renin-angiotensin system. *Cell Tissue Res*. **326** (2), 599-616, (2006).
7. Speth, R., Giese M. Update on the renin-angiotensin system. *J Pharmacol Clin Toxicol*. **1** (1), 1004 (2013).
8. de Kloet, A. D., Liu, M., Rodriguez, V., Krause, E. G., & Sumners, C. Role of neurons and glia in the CNS actions of the renin-angiotensin system in cardiovascular control. *Am J Physiol Regul Integr Comp Physiol*. (2015).
9. Saavedra, J. M., Sanchez-Lemus, E., & Benicky, J. Blockade of brain angiotensin II AT1 receptors ameliorates stress, anxiety, brain inflammation and ischemia: Therapeutic implications. *Psychoneuroendocrinology*. **36** (1), 1-18, (2011).
10. Stornetta, R. L., Hawelu-Johnson, C. L., Guyenet, P. G., & Lynch, K. R. Astrocytes synthesize angiotensinogen in brain. *Science*. **242** 1444-1446 (1988).
11. Li, W., Peng, H., Seth, D. M., & Feng, Y. The Prorenin and (Pro)renin Receptor: New Players in the Brain Renin-Angiotensin System? *Int.J.Hypertens*. **2012**, 290635 (2012).
12. Strittmatter, S. M., Kapiloff, M. S., & Snyder, S. H. [3H]captopril binding to membrane associated angiotensin converting enzyme. *Biochem. Biophys. Res. Commun*. **112**, 1027-1033 (1983).
13. Bild, W., Hritcu, L., Stefanescu, C., & Ciobica, A. Inhibition of central angiotensin II enhances memory function and reduces oxidative stress status in rat hippocampus. *Prog Neuropsychopharmacol Biol Psychiatry*. **43** 79-88, (2013).
14. Wright, J. W., & Harding, J. W. Brain renin-angiotensin-A new look at an old system. *Progress in Neurobiology*. **95** (1), 49-67, (2011).

15. Tashev, R., & Stefanova, M. Hippocampal asymmetry in angiotensin II modulatory effects on learning and memory in rats. *Acta Neurobiol Exp (Wars)*. **75** (1), 48-59 (2015).
16. Reudelhuber, T. L. The continuing saga of the AT2 receptor: a case of the good, the bad, and the innocuous. *Hypertension*. **46** (6), 1261-1262, (2005).
17. Carey, R. M. Cardiovascular and renal regulation by the angiotensin type 2 receptor: the AT2 receptor comes of age. *Hypertension*. **45** (5), 840-844, (2005).
18. Valero-Esquitino, V. *et al.* Direct angiotensin type 2 receptor (AT2R) stimulation attenuates T-cell and microglia activation and prevents demyelination in experimental autoimmune encephalomyelitis in mice. *Clin Sci (Lond)*. **128** (2), 95-109, (2015).
19. Chen, J. *et al.* Neuronal over-expression of ACE2 protects brain from ischemia-induced damage. *Neuropharmacology*. **79c** 550-558, (2014).
20. Kalra, J., Prakash, A., Kumar, P., & Majeed, A. B. Cerebroprotective effects of RAS inhibitors: Beyond their cardio-renal actions. *J Renin Angiotensin Aldosterone Syst.* (2015).
21. Zhao, Y. *et al.* Activation of intracellular angiotensin AT(2) receptors induces rapid cell death in human uterine leiomyosarcoma cells. *Clin Sci (Lond)*. **128** (9), 567-578, (2015).
22. Gehlert, D. R., Speth, R. C., & Wamsley, J. K. Quantitative autoradiography of angiotensin II receptors in the SHR brain. *Peptides*. **7** (6), 1021-1027 (1986).
23. Mendelsohn, F. A., Quirion, R., Saavedra, J. M., Aguilera, G., & Catt, K. J. Autoradiographic localization of angiotensin II receptors in rat brain. *Proc Natl Acad Sci U S A*. **81** (5), 1575-1579 (1984).
24. Gehlert, D. R., Speth, R. C., & Wamsley, J. K. Autoradiographic localization of angiotensin II receptors in the rat brain and kidney. *Eur J Pharmacol*. **98** (1), 145-146 (1984).
25. Speth, R. C. *et al.* Angiotensin II receptor localization in the canine CNS. *Brain Res*. **326** (1), 137-143 (1985).
26. Santos, R. A. S. *et al.* Angiotensin-(1-7) is an endogenous ligand for the G protein-coupled receptor Mas. *Proc Natl Acad Sci U S A*. **100** (14), 8258-8263, (2003).
27. Karamyan, V. T., Gembardt, F., Rabey, F. M., Walther, T., & Speth, R. C. Characterization of the brain-specific non-AT(1), non-AT(2) angiotensin binding site in the mouse. *Eur J Pharmacol*. **590** (1-3), 87-92, (2008).
28. Karamyan, V. T., & Speth, R. C. Distribution of the non-AT1, non-AT2 angiotensin-binding site in the rat brain: preliminary characterization. *Neuroendocrinology*. **88** (4), 256-265, (2008).
29. Karamyan, V. T., Stockmeier, C. A., & Speth, R. C. Human brain contains a novel non-AT1, non-AT2 binding site for active angiotensin peptides. *Life Sci*. **83** (11-12), 421-425, (2008).
30. Miller-Wing, A. V. *et al.* Central angiotensin IV binding sites: distribution and specificity in guinea pig brain. *J Pharmacol Exp Ther*. **266** (3), 1718-1726 (1993).
31. Castren, E., Kurihara, M., & Saavedra, J. M. Autoradiographic localization and characterization of angiotensin II binding sites in the spleen of rats and mice. *Peptides*. **8** (4), 737-742 (1987).
32. MacGregor, D. P. *et al.* Angiotensin II receptor subtypes in the human central nervous system. *Brain Res*. **675** (1-2), 231-240 (1995).
33. Plunkett, L. M., Correa, F. M. A., & Saavedra, J. M. Quantitative autoradiographic determination of angiotensin-converting enzyme binding in rat pituitary and adrenal glands with 125I-351/A, a specific inhibitor. *Regul Pept*. **12** 263-272 (1985).
34. Armando, I. *et al.* Increased angiotensin II AT(1) receptor expression in paraventricular nucleus and hypothalamic-pituitary-adrenal axis stimulation in AT(2) receptor gene disrupted mice. *Neuroendocrinology*. **76** (3), 137-147, (2002).
35. Speth, R. C., & Harding, J. W. in *Angiotensin Protocols* Vol. 51 *Methods in Molecular Medicine*. (ed D. H. Wang) 275-295 Humana Press, (2001).
36. Widdop, R. E., Jones, E. S., Hannan, R. E., & Gaspari, T. A. Angiotensin AT2 receptors: cardiovascular hope or hype? *Br J Pharmacol*. **140** (5), 809-824, (2003).
37. Michel, M. C., Wieland, T., & Tsujimoto, G. How reliable are G-protein-coupled receptor antibodies? *Naunyn Schmiedebergs Arch.Pharmacol*. **379** (4), 385-388 (2009).
38. Jensen, B. C., Swigart, P. M., & Simpson, P. C. Ten commercial antibodies for alpha-1-adrenergic receptor subtypes are nonspecific. *Naunyn Schmiedebergs Arch Pharmacol*. **379** (4), 409-412, (2009).
39. Jositsch, G. *et al.* Suitability of muscarinic acetylcholine receptor antibodies for immunohistochemistry evaluated on tissue sections of receptor gene-deficient mice. *Naunyn Schmiedebergs Arch Pharmacol*. **379** (4), 389-395, (2009).
40. Hamdani, N., & van der Velden, J. Lack of specificity of antibodies directed against human beta-adrenergic receptors. *Naunyn Schmiedebergs Arch Pharmacol*. **379** (4), 403-407, (2009).
41. Bodei, S., Arrighi, N., Spano, P., & Sigala, S. Should we be cautious on the use of commercially available antibodies to dopamine receptors? *Naunyn Schmiedebergs Arch Pharmacol*. **379** (4), 413-415, (2009).
42. Lu, X., & Bartfai, T. Analyzing the validity of GalR1 and GalR2 antibodies using knockout mice. *Naunyn Schmiedebergs Arch Pharmacol*. **379** (4), 417-420, (2009).
43. Everaerts, W. *et al.* Where is TRPV1 expressed in the bladder, do we see the real channel? *Naunyn Schmiedebergs Arch Pharmacol*. **379** (4), 421-425, (2009).
44. Adams, J. M., McCarthy, J. J., & Stocker, S. D. Excess dietary salt alters angiotensinergic regulation of neurons in the rostral ventrolateral medulla. *Hypertension*. **52** (5), 932-937, (2008).
45. Herrera, M., Sparks, M. A., Alfonso-Pecchio, A. R., Harrison-Bernard, L. M., & Coffman, T. M. Lack of specificity of commercial antibodies leads to misidentification of Angiotensin type 1 receptor protein. *Hypertension*. **61** (1), 253-258 (2013).
46. Rateri, D. L. *et al.* Endothelial Cell-Specific Deficiency of Ang II Type 1a Receptors Attenuates Ang II-Induced Ascending Aortic Aneurysms in LDL Receptor(-/-) Mice. *Circ Res*. **108** (5), 574-U583, (2011).
47. Benicky, J., Hafko, R., Sanchez-Lemus, E., Aguilera, G., & Saavedra, J. M. Six Commercially Available Angiotensin II AT(1) Receptor Antibodies are Non-specific. *Cell Mol Neurobiol*. **32** (8), 1353-1365, (2012).
48. Elliott, K. J., Kimura, K., & Eguchi, S. Lack of specificity of commercial antibodies leads to misidentification of angiotensin type-1 receptor protein. *Hypertension*. **61** (4), e31, (2013).
49. Hafko, R. *et al.* Commercially available angiotensin II At(2) receptor antibodies are nonspecific. *PLoS One*. **8** (7), e69234, (2013).
50. Gonzalez, A. D. *et al.* Distribution of angiotensin type 1a receptor-containing cells in the brains of bacterial artificial chromosome transgenic mice. *Neuroscience*. **226** 489-509 (2012).